Studi Trent. Sci. Nat., Acta Geol., 80 (2003): 71-83 ISSN 0392-0534

Open-system alpine speleothems: implications for U-series dating and paleoclimate reconstructions

Andrea BORSATO[1*], Yves QUINIF[2], Alfredo BINI[3] & Yuri DUBLYANSKY

[1]Museo Tridentino di Scienze Naturali, Via Calepina 14, I-38100 Trento
[2]CERAK, Faculté Polytechnique, Rue de Houdain 9, B-7000 Mons
[3]Dipartimento Scienze della Terra, Università degli Studi, Via Mangiagalli 14, I-20133 Milano
[*]E-mail dell'Autore per la corrispondenza: *borsato@mtsn.tn.it*

SUMMARY - *Open-system alpine speleothems: implications for U-series dating and paleoclimate reconstructions* - The present work is a critical review of 130 alpha-spectrometric U/Th analyses of speleothems from north-eastern Italy. About 33% of measurements display activity ratios ($^{230}Th/^{234}U$)>1 while maintaining ($^{234}U/^{238}U$) close to unity, thus falling outside the closed system U-series disequilibrium field. The open-system behaviour was mostly observed in speleothems that, based on geological data and petrographic observations, have experienced dramatic environmental changes, such as flooding of caves by glacial meltwater or dissolution by undersaturated waters. The paper discusses possible causes of the open-system behaviour in the U-Th system, and evaluates evidence for the U leaching *vs.* ^{230}Th introduction. By considering only samples which do not show the open-system behaviour and are not contaminated by detrital thorium, five periods of active speleothem deposition have been identified for north-eastern Italy: 0 to 10 ka, 40 to 63 ka, 88 to 100 ka, 140 to 160 ka, and 190 to 250 ka. Even in these, apparently good, data set, the ages of 140 to 160 ka might be affected by undetected ^{230}Th introduction, since they appear to be 20 to 40 ka older than the data obtained for the same paleoclimate period from European speleothems.

RIASSUNTO - *Speleotemi di sistema aperto in grotte alpine: implicazioni per datazioni della serie dell'uranio e ricostruzioni paleoclimatiche* - Il presente lavoro è la revisione critica di 130 analisi U/Th effettuate in spettrometria alfa su speleotemi dell'Italia nord-orientale. Circa il 33% delle analisi presenta rapporti ($^{230}Th/^{234}U$)>1, pur mantenendo il rapporto ($^{234}U/^{238}U$) vicino all'unità, e cade perciò al di fuori dei valori possibili per il decadimento radioattivo della serie U/Th, testimoniando l'apertura del sistema. In base a dati geologici e osservazioni petrografiche le condizioni di sistema aperto si osservano più comunemente in speleotemi che sono incorsi in drastiche modificazioni ambientali, quali l'allagamento della cavità da parte di acque di fusione glaciale o la dissoluzione da parte di acque sottosature. Il lavoro discute inoltre le possibili cause dell'apertura del sistema per gli isotopi delle serie dell'uranio, e confronta le evidenze di lisciviazione dell'U con quelle di introduzione di ^{230}Th. Considerando solamente i campioni ritenuti affidabili, che non cadono cioè nel campo del sistema aperto, e non sono contaminati da Th detritico, sono stati individuati cinque periodi di formazione per gli speleotemi in Italia nord-orientale: 0-10 ka, 40-63 ka, 88-100 ka, 140-160 ka, e 190-250 ka. In particolare, le analisi che cadono nell'intervallo tra 140 e 160 ka potrebbero essere affette dall'introduzione di ^{230}Th, in quanto appaiono più vecchie di 20-40 ka se confrontate con i dati ottenuti per lo stesso periodo climatico da speleotemi europei.

Key words: U/Th dating, speleothems, U-leaching, paleoclimate
Parole chiave: datazione U/Th, speleotemi, Uranio, paleoclima

1. INTRODUCTION

The U-series disequilibrium dating is a well established method to obtain ages of both organic and inorganic carbonates that are used in paleoclimate reconstructions. The morphology, trace-element and isotope geochemistry, as well as inferred growth rates of speleothems (cave secondary mineral deposits), have been extensively used to gain information on past climate and environments (Harmon *et al.* 1975; Ford & Williams 1989; Gordon *et al.* 1989; Gascoyne 1992; Dorale *et al.* 1992; McDermott *et al.* 1999; Richards

& Dorale 2003). Soundness of interpretations in past climate history studies and in regional correlations of climate events is crucially dependent on the reliability of dating. For example, the correlation between speleothem growth phases and solar insolation maxima for the last half-million years is based solely on the U/Th ages of cave deposits (Henning *et al.* 1983; Cantillana *et al.* 1986; Gordon *et al.* 1989; Maire 1990; Baker *et al.* 1993, Baker *et al.* 1995). The reliability of U-series dating is, therefore, a necessary prerequisite for the paleoclimate studies employing authigenic carbonates.

The basic requirements for age determinations based on the U-series disequilibrium method are: (1) that the specimens contain sufficient amounts of U (typically more than 0.05 ppm); (2) that it is not contaminated by detrital Th; and (3) that the speleothem system has remained "closed" since the time of its formation, meaning that U and products of its decay, particularly ^{230}Th are neither added nor removed from the sample (Cherdyntsev 1971; Gascoyne *et al.* 1978; Ford & Williams 1989).

The "opening" of the system may occur when speleothems are placed in environmental conditions that are substantially different relative to the original precipitation conditions. One example of such process is provided by situation when water moves through the speleothem utilising its internal porosity. This can cause dissolution, dissolution-reprecipitation, and recrystallization of speleothemic material, which results in the change of the speleothem fabrics. Although this change can be detected through optical and scanning electron microscopy, the subject has been largely neglected in paleoclimate research employing continental carbonates (Frisia *et al.* 2000; Frisia *et al.* 2002). Similarly to marine cements, post-depositional mimetic replacement of one carbonate by another can occur in speleothems, and this phenomenon can be detected only through petrographic and microstructural observations (e.g. McDermott *et al.* 1999; Frisia *et al.* 2000; Frisia *et al.* 2002). Virtually any speleothem may have experienced post-depositional recrystallization, which would not necessarily result in development of macroscopic, visually apparent, dissolutional features (e.g., Frisia 1996).

In many Alpine caves, glacial meltwater inundated passages several time in the past, so that the pre-Holocene speleothems underwent possible erosion and dissolution. This is demonstrated by the presence of macroscopic features such as scallops and vugs (Borsato 1995; Frisia *et al.* 1994). Furthermore, flowstones and stalagmites commonly include fine veils consisting of silts and clays interlayered within the carbonates. These veils have either been explained by the wash-in of glaciogenic sediments that formed the infill of epikarstic forms at the surface (Maire 1990), or attributed to the direct inundation of the cave passages by turbid waters. Both the action of glacial meltwater and the mechanical input of sediments may represent natural processes that could disturb the U-Th system in speleothems. The occurrence of such processes would be detrimental from the U-Th dating perspective; potentially, it may render the U-Th ages invalid.

In this paper we analyse the data obtained in the course of 130 alpha-spectrometric analyses of alpine speleothems from north-eastern Italy, and critically revise those analyses that show activity ratios (^{230}Th/^{234}U)[1] that are off the calculated decay field.

2. GEOLOGICAL SETTING, SAMPLES AND METHODS

The analyzed speleothems come from 28 caves in north-eastern Italy: Lombardy region, Trento province and the Dolomites (Fig. 1). The caves, carved in Middle Triassic to Early Jurassic limestones and dolomites (Uggeri 1992; Frisia *et al.* 1994; Borsato 1995) (Tab. 1) developed since the Late Miocene (Uggeri 1992; Uggeri *et al.* 1991; Uggeri *et al.* 1992; Borsato 1995). Altogether, 70 samples of subaerial speleothems (39 flowstones, 27 stalagmites and 4 stalactites) were

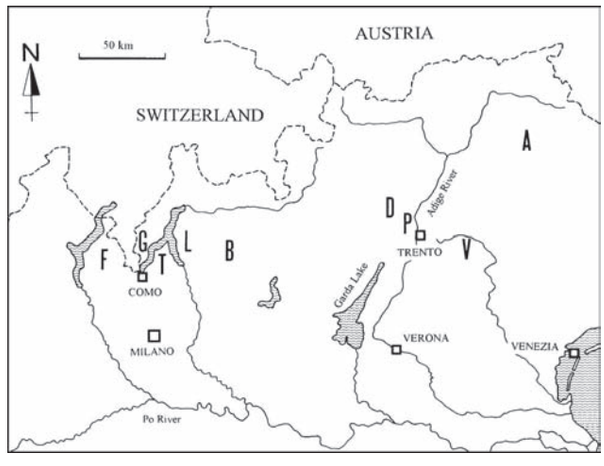

Fig. 1 - Schematic map of northern Italy with the location of the studied karstic areas: A = Altipiani Ampezzani; B = Val Brembana; D = Brenta Dolomites; F = Campo dei Fiori and Valganna; G = Monte Generoso and Monte Bisbino; L = Val di Lori; P = Paganella; T = Pian del Tivano; V = Valsugana.

Fig. 1 - Posizione delle aree carsiche studiate: A = Altipiani Ampezzani; B = Val Brembana; D = Dolomiti di Brenta; F = Campo dei Fiori e Valganna; G = Monte Generoso e Monte Bisbino; L = Val di Lori; P = Paganella; T = Pian del Tivano; V = Valsugana.

[1] In subsequent text, isotopes or isotope ratios in parentheses denote activities or activity ratios, respectively.

Cave	Locality (1)	Elevation (2)	Host rock (3)
Grotta 1100 Gaggi	Paganella (P)	697	DP
Caverna Staloti	Paganella (P)	1535	CG
Abisso Ellesmere	Paganella (P)	1675	CG
Grotta Cesare Battisti	Paganella (P)	1880	CG
Bus de la Spia	Brenta Dolomites (D)	610	CG
Grotta di Collalto	Brenta Dolomites (D)	1000	DP
Grotta del Calgeron	Valsugana (V)	467	DP
Grotta di Ernesto	Valsugana (V)	1167	CG
Grotta di Costalta	Valsugana (V)	1710	DP
Meandro F7 di Fosses	Altipiani Ampezzani (A)	2180	CG
Meandro S2 di Sennes	Altipiani Ampezzani (A)	2220	CG
Grotta di Conturines	Altipiani Ampezzani (A)	2775	DP
Grotta dell'Alabastro	Valganna (F)	510	DS
Bus del Rameron	Campo dei Fiori (F)	720	Mo
Grotta On the Road	Campo dei Fiori (F)	805	Mo
Grotta del Frassino	Campo dei Fiori (F)	900	Mo
Grotta Via col Vento	Campo dei Fiori (F)	1015	Mo
Grotta Marelli	Campo dei Fiori (F)	1027	Mo
Grotta Fontana Marella	Campo dei Fiori (F)	1040	Mo
Grotta Shangai	Campo dei Fiori (F)	1112	Mo
Bucone 1° di Griante	Monte Generoso (G)	708	DP
Grotta Nevera	Monte Generoso (G)	1142	Mo
Grotta Alpe Madrona	Monte Bisbino (G)	900	Mo
Grotta Tacchi	Pian del Tivano (T)	770	Mo
Grotta Capanna Stoppani	Pian del Tivano (T)	1075	Mo
Abisso del Cippei	Pian del Tivano (T)	1200	Mo
Grotta del conglomerato	Val di Lori - Grigna (L)	1200	CQ
La Caerna	Val Brembana (B)	605	CZ

Tab. 1 - Location, and lithology of the studied caves. (1) Location: in bracket the initial of the karstic area as in figure 1; (2) Cave entrance elevation (m a.s.l.); (3) Host rock: DP = Dolomia Principale dolomites (Late Carnian - Norian); CG = Calcari Grigi limestones (Lias); DS = Dolomia di San Salvatore dolomites (Anisian-Ladinian); Mo = Formazione di Moltrasio limestones (Lias); CQ = Quaternary conglomerates; CZ = Calcare di Zu limestones (Raethian).
Tab. 1 - Ubicazione e litologia delle grotte esaminate. (1) Ubicazione: tra parentesi le iniziali delle aree carsiche come in figura 1; (2) Quota di ingresso della cavità (m s.l.m.); (3) Roccia incassante: DP = Dolomia Principale (Carnico Superiore - Norico); CG = Calcari Grigi (Lias); DS = Dolomia di San Salvatore (Anisico-Ladinico); Mo = Formazione di Moltrasio (Lias); CQ = Conglomerati (Quaternario); CZ = Calcare di Zu (Retico).

studied. Speleothems were sliced along the growth axis to study the internal stratigraphy and fabric. Observations were carried out by optical microscopy on thin sections cut both parallel and perpendicular to the growth axis. For 50 samples, micromorphological observations were carried out by scanning electron microscopy (SEM) on freshly broken surfaces, and semi-quantitative minor element analyses were done with SEM-EDAX on polished specimens.

On these 70 samples, 130 alpha-spectrometric analyses were performed at CERAK, Faculté Polytecnique de Mons (Uggeri *et al.* 1991; Uggeri *et al.* 1992; Frisia *et al.* 1994; Borsato 1995; Sauro & Meneghel 1995, Bini *et al.* 1997). From this dataset, 85 analyses were selected for further evaluation (Tab. 2). The selection criteria included relatively high yield of U and Th, leading to lower analytical error in determination of isotope ratios. We excluded all analyses yielding ($^{230}Th/^{232}Th$) < 4, indicating significant contamination by detrital thorium. Such values are typical of the basal flowstones with fine detrital intercalations or porous, calcareous tufa flowstones (Borsato 1995). The average sample size for alpha-spectrometric analysis was 50 g.

3. DISCUSSION OF THE DATA

3.1. Petrographic and morphological observations

All the observed speleothems exhibit four calcite fabrics: microcrystalline, columnar, dendritic and fibrous (for fabric definitions see Frisia *et al.* 2000). Traces of diagenetic phenomena are more intense in specimens that originally consisted of fibrous or dendritic calcite, which posses large surface/volume ratios and are thermodynamically slightly unstable. In these fabrics, the diagenetic phenomena, such as the reorganisation of small individuals into larger domains and the replacement of acicular crystals by patches of equant calcite (Frisia *et al.* 2000) are common and easily recognisable. On the other hand, more stable calcite forms, e.g. columnar, can either be primary or reflect the progressive aggradation of crystallites by dissolution-reprecipitation (Frisia *et al.* 1994; Frisia *et al.* 2000). In this case, identification of diagenetic effects becomes more difficult and requires electron microscopy techniques (Frisia *et al.* 2000).

SEM-EDAX analyses reveal that all the specimens consist of low-magnesium calcite, with a mean $MgCO_3$ content ranging from 0.1 to 0.8 mole % in the case of limestone host rock, and from 0.9 to 2.6 mole % in the case of dolomite host rock (Frisia *et al.* 1994; Borsato 1995). Low-Mg calcite is a stable carbonate form, not prone to recrystallisation unlike the high-Mg calcite and aragonite (Frisia 1996, Frisia *et al.* 2002). Therefore, diagenetic modifications of

Ref (a)	Cave	Sample	U (ppm)	(^{234}U/^{238}U)	(^{230}Th/^{234}U)	(^{230}Th/^{232}Th)	(^{234}U/^{238}U) initial	Age (ka)
1	Grotta 1100 Gaggi	GA-3b	1.558 ±0.015	0.948 ±0.012	0.759 ±0.013	6	0.920	**158.1** [+7.5/-6.6]
1	Caverna Staloti	ST1-1	4.599 ±0.074	1.009 ±0.012	1.394 ±0.028	157		**Open system**
1	Caverna Staloti	ST1-2	5.323 ±0.081	0.988 ±0.011	1.625 ±0.051	224		**Open system**
1	Abisso Ellesmere	AB754	0.122 ±0.003	1.116 ±0.029	0.665 ±0.031	13	1.161	**115.5** [+/-9.4]
1	Grotta Cesare Battisti	CB39	0.243 ±0.004	1.098 ±0.024	0.612 ±0.035	25	1.131	**100.8** [+10.4/-9.5]
1	Grotta Cesare Battisti	CB17	0.149 ±0.004	1.094 ±0.045	1.387 ±0.168	9		**Open system**
1	Bus de la Spia	BS17-a	0.149 ±0.005	1.080 ±0.048	0.905 ±0.095	14	1.157	**237.4** [+180/-75]
1	Bus de la Spia	BS17-c	0.199 ±0.005	1.060 ±0.031	1.276 ±0.061	14		**Open system**
1	Bus de la Spia	BS17-d	0.160 ±0.003	1.122 ±0.029	0.875 ±0.026	16	1.219	**208.0** [+24.0/-19.1]
1	Bus de la Spia	BS12	0.275 ±0.011	0.997 ±0.038	0.821 ±0.034	6	0.994	**187.0** [+30.1/-22.1]
1	Bus de la Spia	BS7-9	0.194 ±0.009	1.054 ±0.056	1.419 ±0.142	19		**Open system**
1	Bus de la Spia	BS7-8	0.295 ±0.012	0.999 ±0.037	0.761 ±0.042	8	0.998	**155.7** [+36/-28]
1	Bus de la Spia	BS7-6	0.192 ±0.008	1.051 ±0.053	0.959 ±0.048	10	1.124	**313.9** [+inf./-78]
1	Bus de la Spia	BS7-4	0.252 ±0.013	0.955 ±0.052	0.761 ±0.046	6	0.929	**158.7** [+52/-36]
1	Bus de la Spia	BS7-1	0.207 ±0.011	1.011 ±0.059	1.415 ±0.097	11		**Open system**
1	Grotta di Collalto	CL11	0.733 ±0.070	1.072 ±0.080	1.540 ±0.160	44		**Open system**
1	Grotta di Collalto	CL9a	0.985 ±0.024	1.008 ±0.017	0.392 ±0.083	19	1.009	**54.0** [+16/-14]
1	Grotta di Collalto	CL9b	1.019 ±0.036	0.972 ±0.024	0.687 ±0.028	5	0.880	**127.1** [+11.7/-10.3]
1	Grotta di Collalto	CL9c	0.580 ±0.027	1.031 ±0.036	1.176 ±0.245	8		**Open system**
1	Grotta di Collalto	CL8	0.374 ±0.005	1.056 ±0.015	0.894 ±0.016	17	1.106	**231.7** [+18.1/-15.1]
1	Grotta del Calgeron	CN31-2	0.103 ±0.021	1.931 ±0.378	0.112 ±0.025	7	1.965	**12.9** [+3.1/-3.0]
1	Grotta del Calgeron	CN31-3	0.176 ±0.007	1.715 ±0.072	0.152 ±0.013	4	1.752	**17.7** [+/-1.6]
1	Grotta di Ernesto	ER8b	0.042 ±0.004	1.710 ±0.205	0.291 ±0.034	4	1.786	**36.4** [+5/-5]
1	Grotta di Ernesto	ER20b	0.034 ±0.001	1.349 ±0.068	0.585 ±0.033	12	1.450	**90.9** [+8.8/-8.0]
1	Grotta di Ernesto	ER28-7	0.062 ±0.002	2.137 ±0.083	0.832 ±0.041	28	2.743	**152.3** [+15.9/-14]
1	Grotta di Ernesto	ER30-1	0.028 ±0.001	2.002 ±0.099	0.797 ±0.036	13	2.495	**142.8** [+13.4/-11.9]
1	Grotta di Ernesto	ER30-3	0.028 ±0.001	1.828 ±0.082	0.827 ±0.034	17	2.280	**155.4** [+14.8/-12.9]
1	Grotta di Costalta	CS6-3	0.087 ±0.004	1.088 ±0.067	1.557 ±0.112	7		**Open system**
1	Grotta di Costalta	CS6-1	0.109 ±0.004	1.096 ±0.054	1.799 ±0.112	13		**Open system**
2	M. F7 Alpe di Fosses	D-02	0.043 ±0.003	1.073 ±0.122	1.281 ±0.190	24		**Open system**
2	M. F7 Alpe di Fosses	D-03	0.057 ±0.007	1.507 ±0.237	0.706 ±0.090	7	1.712	**120.6** [+36.4/-35.4]
2	M. S2 di Sennes	Bin-01	0.156 ±0.003	1.054 ±0.031	0.910 ±0.031	226	1.109	**246.3** [+48.4/-31.8]
3	Grotta di Conturines	B2-1	0.182 ±0.003	1.005 ±0.021	1.625 ±0.111	64		**Open system**
3	Grotta di Conturines	B2-2	0.155 ±0.002	1.036 ±0.019	1.571 ±0.129	65		**Open system**
3	Grotta di Conturines	CO-C1	0.184 ±0.002	1.055 ±0.017	1.235 ±0.066	163		**Open system**
3	Grotta di Conturines	CO-C2	0.260 ±0.002	1.008 ±0.018	1.202 ±0.138	>1000		**Open system**
3	Grotta di Conturines	CO-C3	0.192 ±0.002	1.020 ±0.011	1.336 ±0.215	>1000		**Open system**
3	Grotta di Conturines	CO-C4	0.213 ±0.003	1.046 ±0.017	1.209 ±0.067	47		**Open system**
4, 6	Grotta dell'Alabastro	AB-737	0.432 ±0.015	1.222 ±0.056	0.885 ±0.050	9	1.394	**204.8** [+45.2/-30.8]
4, 6	Grotta dell'Alabastro	AL-10	0.386 ±0.004	1.030 ±0.013	0.444 ±0.037	27	1.036	**63.4** [+7.7/-7.0]
4, 6	Grotta dell'Alabastro	AL-11	0.423 ±0.005	1.008 ±0.011	0.383 ±0.011	48	1.010	**52.3** [+2.1/-2.0]
4, 6	Grotta dell'Alabastro	AL-12	0.712 ±0.012	1.028 ±0.014	0.049 ±0.004	5	1.029	**5.5** [+0.4/-0.5]
4, 6	Grotta dell'Alabastro	AL-13	5.507 ±0.128	0.995 ±0.008	0.015 ±0.001	8	0.995	**1.6** [+/-0.1]
4, 6	Grotta dell'Alabastro	AL-14	0.936 ±0.016	0.981 ±0.012	0.060 ±0.002	32	0.981	**6.8** [+/-0.2]
4, 6	Grotta dell'Alabastro	AL-17(1)	0.389 ±0.004	1.021 ±0.011	0.343 ±0.008	16	1.024	**45.6** [+1.3/-1.4]
4, 6	Grotta dell'Alabastro	AL-17(2)	0.310 ±0.008	1.013 ±0.026	0.379 ±0.018	5	1.015	**51.7** [+/-3.2]
4, 6	Bus del Rameron	RE-2	2.000 ±0.033	1.907 ±0.020	0.587 ±0.013	181	2.161	**88.1** [+/-2]
4, 6	Gr. On the Road	Marnovelle	0.661 ±0.011	1.022 ±0.018	0.992 ±0.024	61		**Equilibrium**
4, 6	Grotta del Frassino	FR5-1	0.435 ±0.007	1.255 ±0.027	1.119 ±0.031	16		**Open system**
4, 6	Grotta del Frassino	FR7-1	0.213 ±0.006	1.088 ±0.035	1.161 ±0.069	63		**Open system**
4, 6	Grotta del Frassino	FR8-1	0.383 ±0.011	1.017 ±0.035	1.189 ±0.050	53		**Open system**
4, 6	Grotta del Frassino	FR9-2	0.377 ±0.033	1.274 ±0.130	1.303 ±0.208	25		**Open system**
4, 6	Grotta Via col Vento	VV5	0.973 ±0.005	1.003 ±0.005	1.175 ±0.027	61		**Open system**
4, 6	Grotta Via col Vento	VV20	1.637 ±0.023	1.026 ±0.011	1.048 ±0.033	50		**>350**
4, 6	Grotta Marelli	MA20	0.364 ±0.007	1.029 ±0.023	0.860 ±0.044	23	1.056	**229.6** [+55.7/-35.5]
5, 6	Grotta Marelli	MA21	1.297 ±0.048	1.032 ±0.032	0.874 ±0.041	217	1.059	**219.0** [+48.2/-31.8]
5, 6	Grotta Marelli	MA22	0.927 ±0.02	1.036 ±0.021	0.909 ±0.026	69	1.072	**250.0** [+40.2/-38.3]
5, 6	Grotta Marelli	MA24	0.311 ±0.031	0.950 ±0.117	0.991 ±0.115	297		**Equilibrium**
5, 6	Grotta Marelli	A1	1.694 ±0.011	0.994 ±0.005	1.367 ±0.090	28		**Open system**
5, 6	Grotta Marelli	A2	0.743 ±0.028	1.031 ±0.034	1.034 ±0.049	67		**>350**
5, 6	Grotta Marelli	B1 (s)	1.734 ±0.009	1.009 ±0.004	1.107 ±0.087	91		**>350**
5, 6	Grotta Marelli	B1 (b)	1.657 ±0.019	1.014 ±0.009	1.090 ±0.023	223		**>350**
5, 6	Grotta Marelli	C1 (b)	1.702 ±0.005	1.001 ±0.005	0.937 ±0.011	72	1.002	**298.9** [+24/-20]
5, 6	Grotta Marelli	C1 (s)	1.122 ±0.006	1.004 ±0.004	0.922 ±0.025	50	1.009	**275.5** [+43/-30]
5, 6	Grotta Marelli	D1 (b)	1.590 ±0.007	1.007 ±0.004	0.966 ±0.053	36	1.019	**>350**
5, 6	Grotta Marelli	D1 (s)	1.540 ±0.009	1.004 ±0.005	0.988 ±0.013	243		**Equilibrium**
5, 6	Grotta Marelli	H1	1.211 ±0.009	1.001 ±0.006	0.931 ±0.080	18		**>350**
4, 6	Gr. Fontana Marella	AB758	0.259 ±0.014	1.181 ±0.087	1.042 ±0.067	6		**>350**
4, 6	Grotta Shangai	AB-746	0.458 ±0.008	1.020 ±0.018	1.222 ±0.103	20		**Open system**
6	Bucone 1° di Griante	BT9-1	1.181 ±0.011	0.871 ±0.006	0.082 ±0.002	36	0.867	**9.3** [+0.2/-0.3]
6	Bucone 1° di Griante	BT-10	0.494 ±0.016	0.988 ±0.023	0.074 ±0.005	11	0.988	**8.3** [+0.7/-0.6]
6	Grotta Nevera	NE-18a	0.226 ±0.003	2.149 ±0.024	1.022 ±0.040	25	3.272	**242.9** [+31.2/-25.2]
6	Grotta Nevera	NE-18b	0.090 ±0.006	1.591 ±0.130	0.621 ±0.047	11	1.777	**97.4** [+13/-11.3]
6	Grotta Nevera	NE-19	0.216 ±0.003	1.170 ±0.018	0.919 ±0.031	8	1.338	**234.7** [+33/-25.2]
6	Grotta Alpe Madrona	2264(1)	0.284 ±0.009	1.058 ±0.054	1.194 ±0.301	35		**Open system**
6	Grotta Alpe Madrona	2265(1)	0.149 ±0.022	2.189 ±0.338	3.378 ±1.411	12		**Open system**
6	Grotta Alpe Madrona	MAD-ST-1(2)	0.202 ±0.011	0.917 ±0.062	1.411 ±0.227	>1000		**Open system**
6	Grotta Tacchi	Bini14	0.176 ±0.023	1.477 ±0.236	2.520 ±0.403	24		**Open system**
6	Gr. Cap. Stoppani	Bin08	0.285 ±0.007	1.008 ±0.028	0.973 ±0.047	179		**>350**
6	Abisso del Cippei	Bin06	0.187 ±0.008	1.282 ±0.070	0.792 ±0.050	185	1.436	**155.1** [+26/-20.3]
6	Abisso del Cippei	Bin07	0.281 ±0.006	1.384 ±0.032	0.887 ±0.031	383	1.664	**194.8** [+20.7/-17.4]
6	Grotta del conglomerato	BN3935-1	0.258 ±0.005	1.049 ±0.022	0.066 ±0.007	8	1.050	**7.4** [+/-0.9]
6	Grotta del conglomerato	BN3935-2	0.363 ±0.004	1.078 ±0.013	0.061 ±0.005	7	1.080	**6.8** [+0.6/-0.5]
6	La Caerna	AB756	0.554 ±0.011	1.167 ±0.019	0.880 ±0.023	68	1.299	**206.4** [+18.3/-15.5]
6	La Caerna	AB757	0.846 ±0.013	1.606 ±0.019	0.314 ±0.012	66	1.678	**39.8** [+/-1.8]

◀ Tab. 2 - Uranium and thorium isotope data and calculated radiometric ages (errors are quoted as 1 σ). (a) References: 1: Borsato 1995; 2: Sauro & Meneghel 1995; 3: Frisia *et al.* 1994; 4: Uggeri *et al.* 1991; 5: Uggeri *et al.* 1992; 6: Bini *et al.* 1997.
Tab. 2 - Rapporti di attività degli isotopi di uranio e torio ed età radiometriche calcolate (gli errori sono di 1 σ). (a) Riferimenti bibliografici: 1: Borsato 1995; 2: Sauro & Meneghel 1995; 3: Frisia et al. *1994; 4: Uggeri* et al. *1991; 5: Uggeri* et al. *1992; 6: Bini* et al. *1997.*

such calcite could have occurred only in response to important changes of the environmental parameters.

3.2. Open-system samples

About one third of the 85 selected analyses are characterized by (^{230}Th/^{234}U) >1 (Tab. 2). The (^{230}Th/^{234}U) excess in most of the samples ranges between 0.2 and 0.7 (mean 0.35±0.18). In most cases, the respective (^{238}U/^{234}U) values are close to unity rendering these analyses off the calculated decay field (Fig. 2). Such isotope relationships can be caused by either removal of U from, or by introduction of ^{230}Th into the sample: a situation commonly termed "open system" behaviour.

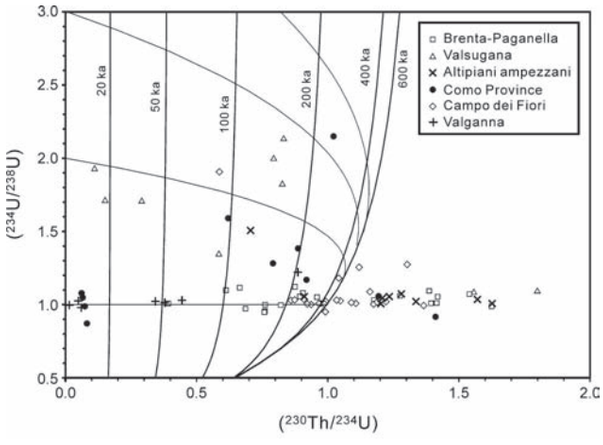

Fig. 2 - (^{234}U/^{238}U) vs. (^{230}Th/^{234}U) diagram for the speleothems from the studied areas (cfr. Tab. 2). Solid-bold lines are isochrones; fine lines show the isotopic evolution with time in a closed system for samples with $(^{234}U/^{238}U)_{initial}$ of 1, 2, 3 and 4 respectively. From this diagram it is possible to calculate graphically the ages for the closed system samples. All data falling to the right of the 600 ka-isochrone reflect open-system behavior. Error bars are omitted for clarity.
Fig. 2 - Grafico dei rapporti di attività ^{234}U/^{238}U - ^{230}Th/^{234}U che illustra la composizione isotopica degli speleotemi studiati nelle diverse aree (cfr. Tab. 2). Le linee spesse sono isocrone, quelle sottili mostrano l'evoluzione dei rapporti isotopici nel tempo in un sistema chiuso per campioni con un rapporto di attività ^{234}U/^{238}U iniziale di 1, 2, 3 e 4 rispettivamente. Dal diagramma è possibile calcolare graficamente le età per campioni di sistema chiuso. Tutti i campioni a destra dell'isocrona di 600 ka sono di sistema aperto. Le barre di errore sono omesse per chiarezza.

The comparison of the U isotopic composition between open- and closed-system samples (Fig. 2) indicates that the open-system samples have (^{234}U/^{238}U) = 1.0 ± 0.1, similar to the values of their closed-system counterparts (e.g., Brenta-Paganella samples).

3.3. General consideration of the open-system behaviour

In figure 3 we illustrate temporal evolution of the U and Th isotope properties of a speleothem, affected by an event, which "opens" the system (i.e., causes removal of U or introduction of ^{230}Th). The figure 3-A and B show trends induced by Th input or U leaching for a sample with $(^{234}U/^{238}U)_{initial}$=1. For the first 20 ka sample develops as a closed system, so that there is steady increase in the (^{230}Th/^{234}U). Then, opening of the system (point 2, bold grey arrow) brings system to the point 3. From this moment on, two processes: decay of the allogenic (or excess) ^{230}Th and *in situ* production of ^{230}Th and its decay begin to compete, finally bringing the sample to the state of equilibrium (^{230}Th/^{234}U) = 1 (point 5). Figure 3-C and D corresponds to two cases of opening of the system for samples with $(^{234}U/^{238}U)_{initial}$=2.5. The case C depicts input of ^{230}Th or removal of U, not associated with selective leaching of ^{234}U. The case D corresponds to the case when ^{234}U is removed from the sample preferentially, so that (^{234}U/^{238}U) decreases in the process.

Isotope data measured in samples that have experienced "opening" during their history should evolve along the trajectories shown in figure 3, so that actual position of the data will be controlled by many factors, including character of system's "perturbation", its extent, as well as time elapsed after the perturbation has taken place.

3.4. Analysis of the U series isotope data

The processes of U leaching or ^{230}Th input would be expected to reveal themselves through a series of geochemical features. In this section we evaluate the data reported in table 2, trying to find out what mechanism, U removal or ^{230}Th input, constitutes the more likely explanation for the observed isotopic disequilibrium (i.e., (^{230}Th/^{234}U)>1). We will do that through the comparison of the closed-system and open-system data sets as a whole, as well as by comparing individual samples from caves in which both closed-sys-

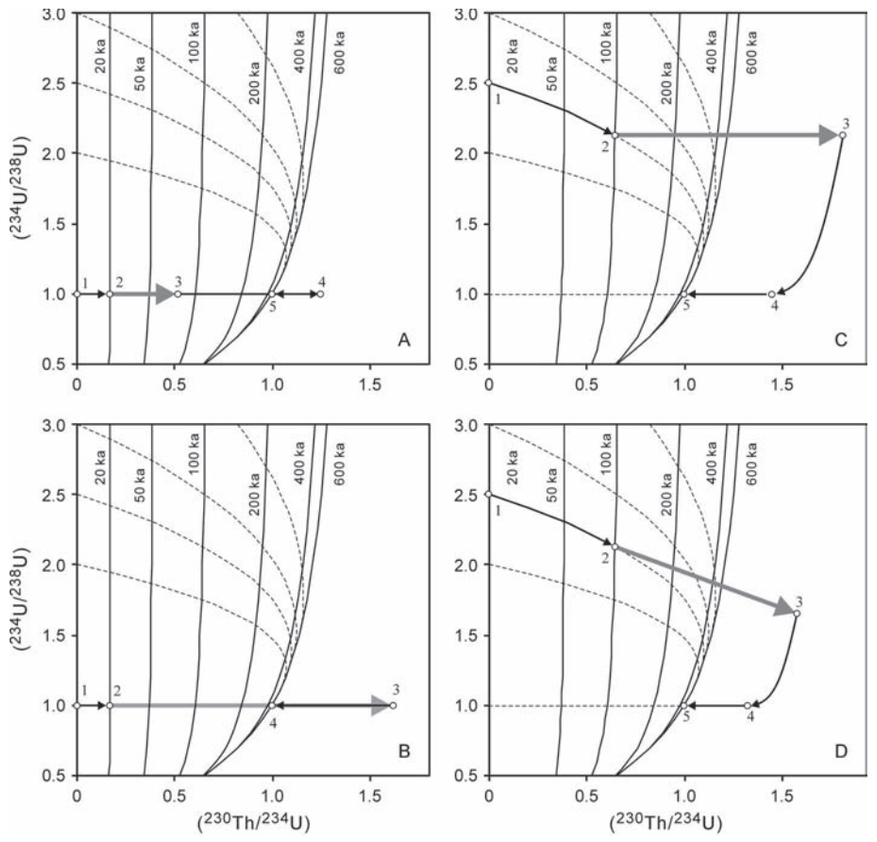

Fig. 3 - Speleothems open-system behaviour models (cfr. Fig. 2). Normal evolution of isotope system, governed by laws of radioactive decay is shown as thin black arrows; bold grey arrows show isotope changes induced by "opening" of the system (i.e. U leaching or ^{230}Th enrichment) that correspond to geologically fast or istantaneous events. Numbered white circles mark characteristic states of the system. Depending on the age of sample, its measured (^{234}U/^{238}U) and (^{230}Th/^{234}U) values should plot somewhere on the trajectory delineated by black arrows.

Fig. 3 - Modello per speleotemi di sistema aperto (cfr. Fig. 2). L'evoluzione guidata dalle sole leggi del decadimento radioattivo è rappresentata da frecce sottili; le frecce grigie più spesse rappresentano variazioni nei rapporti isotopici indotte dall'apertura del sistema (cioè lisciviazione dell'U o arricchimento in ^{230}Th), e corrispondono ad eventi veloci o immediati nella scala geologica. I cerchietti numerati indicano particolari stati nel sistema. A seconda dell'età del campione i valori di (^{234}U/^{238}U) e (^{230}Th/^{234}U) possono cadere in differenti punti lungo le traiettorie delineate dalle frecce.

tem and open-system data were obtained. The latter data are available from 4 caves: Grotta Cesare Battisti, Grotta Collalto, Bus de la Spia, and Grotta Marelli.

3.4.1. Leaching of U from speleothems – theoretical consideration

Leaching of U is considered to be the leading mechanism responsible for the open-system behaviour occasionally observed in speleothems (e.g., Railsback *et al.* 2002). When addressing the possibility of the leaching of U from speleothem, it is important to understand first in what form U can be present in speleothems. U may be incorporated in crystal structure, it may form a separate U-rich mineral phase(s), it may be present in adsorbed state on mineral surfaces and particulate impurities, or it may be associated with organic matter in speleothems. Although the list above is not exhaustive, it likely captures the potentially most important situations. Unfortunately, this issue appears to be a totally unexplored field in karst studies. Some insight can be gained from experimental mineralogical and geochemical studies.

Reeder *et al.* (2001) studied synthetic U-doped calcite (U = 15 to 725 ppm), which was grown in the laboratory at different but generally high supersaturations (SI=0.6-0.8 and 1.4-1.5). The results indicate that U is primarily incorporated into the calcite structure, as uranil ion, and does not form a second phase. Most speleothemic calcites have much lower contents of U than those studied by Reeder *et al.* (2001); for instance, in samples discussed in this paper, U = 0.04 to 2.0 ppm with only 3 outliers at 4.5 to 5.5 ppm. It is likely, therefore, that U in the Trento province

speleothems is incorporated in the structure of the calcite and does not occur as a separate phase. If this assumption is correct, the removal of U from samples would require dissolution of the host calcite. In order to decrease the overall content of U in a sample, say by 10%, it is necessary that 10% of the calcite is dissolved, removed and replaced by equivalent amount of U-free calcite (or, alternatively, 20% of calcite is dissolved and replaced with calcite having U content of 50% that of the "initial" calcite).

Our calculations show that, in order to produce the values of (^{230}Th/^{234}U)>1 reported in table 2, between 4.8% and as much as 89% of U, contained in samples would have to be leached. These are minimum estimates, assuming that the ^{230}Th and ^{234}U were in secular equilibrium before leaching. Such extensive leaching would require practically complete dissolution of the primary calcite and replacement of it with U-free calcite. Petrographic observations do not corroborate this mechanism. Thus, two interpretations are possible: either U leaching is not the dominant process responsible for the observed (^{230}Th/^{234}U)>1, or U in speleothems is not incorporated in the structure of the calcite and is prone to selective leaching.

Due to the lack of the data regarding incorporation of U in real speleothems, the possibility that some U could be adsorbed on the mineral surfaces (e.g., intergranular porosity) can neither be confirmed nor ruled out. A similarly unexplored area is the possible association of U in speleothems with organic matter (organic-rich layers). Late waters seeping through speleothems could partially dissolve this matter and thus remove some U associated with it. These questions require further dedicated studies. Presently, indirect evidence suggests that U in speleothem might be expelled from calcite in the course of recrystallization of the latter, or might be concentrated in the inclusion-rich layers. For example, Railsback *et al.* (2002) reported elevated contents of U associates with zoned inclusion rich calcite, as well as apparent depletion in U of coarsely crystalline (likely recrystallized) columnar calcite crystal as compared with the more finely crystalline ones.

The possible expelling of U from crystal lattice and its concentration in interstices between crystals or in inclusion-rich zones is potentially important. On one hand, it makes U potentially more mobile; on another hand, dissolution and removal of U from such easily accessible sites would not lead to any appreciable fractionation between ^{238}U and ^{234}U, related to alpha-decay processes.

3.4.2. Evidence on the removal of uranium

The hypothesis about leaching of U from studied samples would be supported if the U contents in the closed-system samples were found to be generally

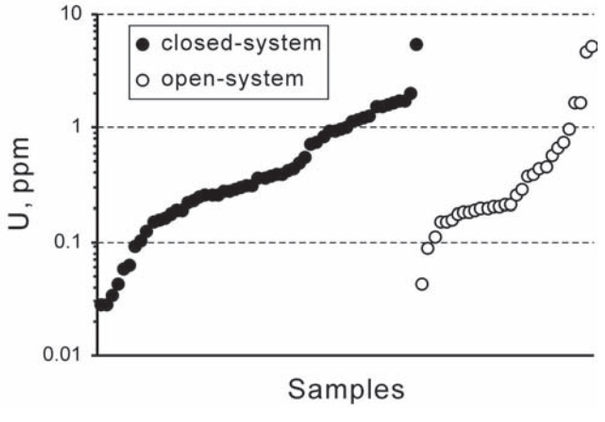

Fig. 4 - Contents of U in closed- and open-system samples (data from Tab. 2). For most samples error bars are less than the size of the symbol.

Fig. 4 - Contenuto in U per campioni di sistema chiuso ed aperto (dati da Tab. 2). Per gran parte dei campioni le barre di errore sono inferiori alla grandezza del simbolo.

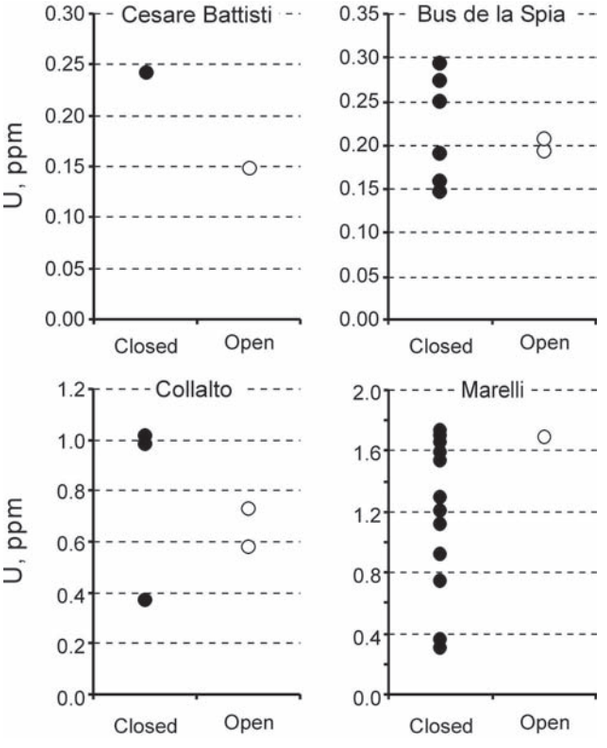

Fig. 5 - Comparison of U contents in samples from the same caves, data from which show both closed- and open-system behavior (data from Tab. 2).

Fig. 5 - Confronto tra contenuto di U in campioni di sistema chiuso ed aperto (dati da Tab. 2) in alcune delle grotte studiate.

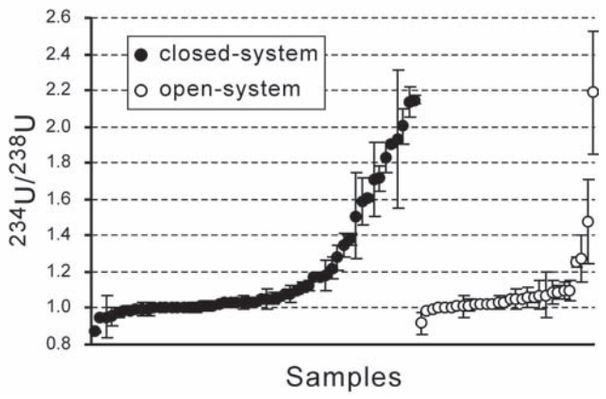

Fig. 6 - Comparison of the ($^{234}U/^{238}U$) values from the closed-system and the open-system samples (data from Tab. 2; error bar is 1σ).
Fig. 6 - Confronto tra valori ($^{234}U/^{238}U$) in campioni di sistema chiuso ed aperto (dati da Tab. 2; barre di errore 1σ).

greater than those in the open system ones. In figure 4 we compare U contents in closed- and open-system samples. It is apparent from the figure that the contents of U in both data sets are similar. Thus, no overall depletion in U is apparent for the open-system samples.

In individual samples from which both closed- and open-system data were obtained, the open-system subsamples also do not show any systematic depletion in U relative to their closed-system counterparts (Fig. 5). Although in one sample some depletion can be seen (Cesare Battisti), the U contents in three other samples are similar.

Because dissolution of U from rocks is commonly associated with preferential removal of ^{234}U related to recoil processes (Fleischer 1980; Osmond & Cowart 1982), activity ratios ($^{234}U/^{238}U$) in U-leached samples would be expected to be less than in closed-system ones (in some cases they may become <1).

In figure 6 we compare ($^{234}U/^{238}U$) values measured in closed- and open-system samples. The values for both types of samples, however, appear to be similar, with most values falling near unity (i.e., secular equilibrium). In both data sets there are values substantially greater than unity (suggesting ages younger than roughly 500 ka), as well as single values smaller than unity (suggesting preferential removal of ^{234}U from samples). Thus, on the broad scale, there is no evidence that the open-system samples suffered preferential removal of ^{234}U any more than the closed-system samples ones.

Summarizing, the available data on U and U-isotope contents in studied calcite do not lend direct support to the hypothesis of the post-depositional removal of U as the major cause for the open-system character of samples.

3.4.3. Mobilization of Th in karst water and its migration – theoretical consideration

Th is commonly perceived as an element which is practically insoluble and immobile in aqueous solutions. As a result, the possibility of Th mobility in the cave environment is *a priori* rejected and is not considered when evaluating possible causes of the open-system behaviour of speleothems (e.g., Railsback *et al.* 2002). Yet, measurable amounts of Th are found in natural groundwaters and other indications of Th mobility, reflected, for example, by unreasonably old U-Th ages measured in modern speleothems have recently been reported (Whitehead *et al.* 1999). Activity ratios ($^{230}Th/^{232}Th$) ranging from 1 to as much as 1000 have been reported from limestone groundwaters (Ivanovich & Alexander 1987). This likely reflects supply of ^{230}Th into water by α-recoil mechanisms and requires substantial Th mobility in carbonate groundwaters.

As it is described in Bourdon *et al.* 2003, α-recoil has a three-fold effect on the fate of the daughter nuclides: (1) the recoil atom may be ejected from the site where it was located directly in the adjacent phase (water); (2) the site is damaged by α-particle which makes the daughter prone to subsequent mobilization; and (3) the atom is displaced from its original location and thus can also be more easily removed.

The process (1) has purely physical nature and does not depend on the solubility of a given nuclide. Fleisher & Raabe (1975) defined the number of daughter nuclides that can be ejected from mineral grains per unit of time:

$$R_N = \rho_s (1-\phi) \frac{r^3 - (r-\delta)^3}{4r^3} \lambda N$$

where ϕ is the porosity, ρ_s is the density of the rock, r is the grain size, δ is the range (displacement distance for recoiling nuclide in solid phase, approximately 40 nm), λ is the decay constant of a parent, and N is the number of atoms per unit of mass of the parent nuclide.

Most of the bedrocks in which caves develop are sufficiently old, so that the U decay series in them have reached secular equilibrium. It is apparent from the equation above that in such rocks, the amounts of ^{234}U and ^{230}Th that can be ejected directly into the pore waters due to recoil of their parents will be the same (even though their respective parents, ^{238}U and ^{234}U have different λ and N, the products of the latter, activities, are equal).

The processes (2) and (3) operate through dissolution of the damaged part of the crystal lattice surrounding the displaced atom and dissolution (hydration) of the nuclide atom. Again, dissolution of the damaged crystal does not depend on the nature of the radionuclide and thus should be similar for the sites containing atoms of ^{234}U and ^{230}Th. Because the hydration of the nuclides is

controlled by their solubilities, at this stage the behaviour of U and Th becomes drastically dissimilar. U^{6+} is relatively soluble and exists in oxidizing solutions as uranil ion $(UO_2)^{2+}$. Thus, ^{234}U may be readily dissolved and carried out of the system. The cumulative action of ejection, mineral dissolution and U mobilization is believed to be responsible for $(^{234}U/^{238}U)>1$ universally observed in natural groundwaters.

Chemical solubility of Th in pure water is extremely low except at very low pH. It can be enhanced by the presence of common inorganic ligands (F^-, Cl^-, PO_4^{3-}, CO_3^{2-}) below pH 6 and by presence of organic ligands (e.g., humic and fulvic acids) up to pH 8 (Langmuir & Herman 1980). In addition, Th is readily absorbed on surfaces of the minerals and on colloidal particles. These two absorption schemes may have the opposite effects on Th mobility: adsorption on mineral surfaces tends to render Th immobile, whereas colloidal particles are increasingly known as effective carriers capable of transporting radionuclides with very low chemical solubility (e.g., Kersting *et al.* 1999).

Organic acids are well known constituents in speleothems (White & Brennan 1989; Lauritzen *et al.* 1986; Shopov *et al.* 1994; Hill & Forti 1997; Ramseyer *et al.* 1997) which implies their presence in the carbonate groundwaters. Waters that have passed through soils could, thus, become efficient carriers of Th. Annual variability of the organic acid contents in percolating waters opens the possibility that the Th transport might also be season-sensitive.

Besides recoil mechanisms, Th might be supplied to the cave water by chemical dissolution of the bedrock, as well as introduced in adsorbed state on allogenic particulate matter. The "fingerprint" of such a process would be a high proportion of the ^{232}Th, and respectively, low $(^{230}Th/^{232}Th)$ ratios. In contrast, high $(^{230}Th/^{232}Th)$ ratios measured in some speleothems (>1000, see Tab. 2) may reflect situation in which chemical weathering of the bedrock is low (i.e., waters are close to equilibrium) so that little detrital ^{232}Th is supplied into the waters by dissolution of the bedrock, whereas ^{230}Th is preferentially supplied by "physical" recoil mechanisms which do not depend on the chemistry of water.

3.4.4. Evidence on the introduction of thorium

The hypothesis about introduction of Th into the samples would be supported if the contents of ^{230}Th, in open-system samples, were found to be greater than those in closed-system ones. An internal check for this criterion would be the absence of the concomi-

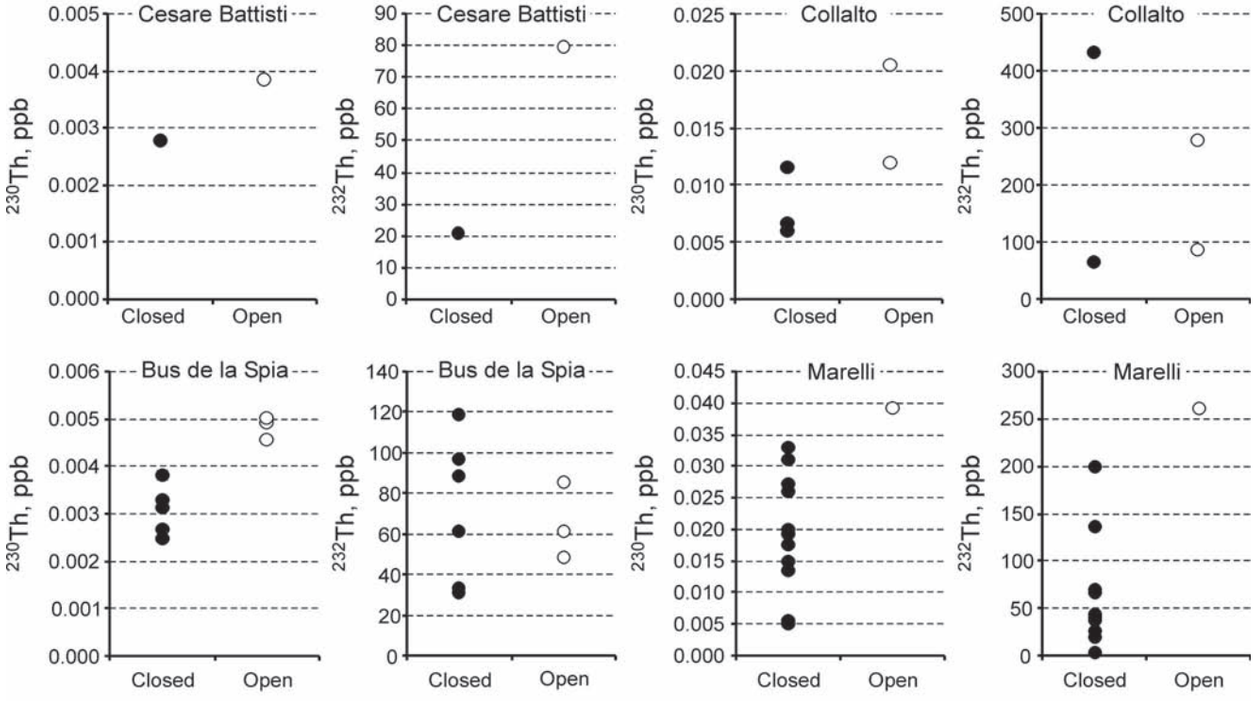

Fig. 7 - Comparison of the ^{230}Th and ^{232}Th contents in closed- and open-system samples (data from Tab. 2). Note that for Collalto and Bus de la Spia caves elevated contents of radiogenic ^{230}Th are not accompanied by the increase in "detrital" ^{232}Th contents.
Fig. 7 - Confronto tra contenuti in ^{230}Th e ^{232}Th in campioni di sistema chiuso ed aperto (dati da Tab. 2). Si noti che nei campioni della Grotta di Collalto e del Bus de la Spia elevate concentrazioni di ^{230}Th radiogenico non corrispondono ad un incremento in ^{232}Th "detritico".

tant increase in ^{232}Th contents in such samples, which would indicate that the excess ^{230}Th is unrelated to the overall detrital Th contamination.

The contents of ^{230}Th and ^{232}Th in closed- and open-system samples are shown in figure 7. Importantly, the contents of ^{230}Th are elevated in all open-system calcites relative to the calcite from the same caves that seem to be "closed". In samples from two caves, Cesare Battisti and Marelli, the increased contents of radiogenic ^{230}Th are accompanied by the increase in "detrital" ^{232}Th contents. For these samples interpretation is ambiguous, since the ^{230}Th could have been introduced along with the "detrital" thorium. However, in samples from two other caves, Collalto and Bus de la Spia, the ^{230}Th contents in the open-system calcite are increased without concomitant increase in the ^{232}Th, which remains at the levels typical of the closed-system calcite. This strongly suggests the selective input of the ^{230}Th into these speleothems.

It must be emphasized, that the absolute amounts of ^{230}Th that would need to be introduced into studied samples in order to produce the observed distortion of the isotope record are quite small. For example, if original calcite sample contains $4 \cdot 10^{-3}$ ppb of ^{230}Th (a typical value for our samples), it is sufficient to increase concentration by only ca. $8 \cdot 10^{-4}$ ppb to obtain the measured excesses of the (^{230}Th/^{234}U). Such tiny amounts of Th may easily be incorporated into the porosity of the speleothemic samples. This contrasts strongly with uranium, for which $1.6 \cdot 10^{-2}$ to 5.5 ppm would have to be removed, along with 4.8% to 89% of the host calcite.

3.5. Causes of the open-system behaviour in speleothems from north-eastern Italy

Morphological and sedimentological studies (Bini & Uggeri 1992; Uggeri 1992; Frisia *et al.* 1994; Borsato 1995) have shown that several caves fed by subglacial streams during glacial and late-glacial stages were flooded by turbulent meltwaters, as indicated by surface scallops and fluted hypogean karren on speleothems and cave walls. These erosive morphologies are typical of caves located near the valley bottoms and below the maximum elevation reached by the Last Glacial Maximum (LGM) glaciers. Examples of such caves are Bus de la Spia, Grotta del Calgeron and Grotta Tacchi (Tab. 1).

In all caves above the timberline (~1,900 m above sea level), the present-day seepage waters are undersaturated with respect to calcite (Borsato 1995) so that calcite deposition does not occurs, and ancient speleothems can undergo dissolution. Limited surface dissolution phenomena in fossil speleothems were also observed in caves developed between the timberline and the present-day deciduous forest upper limit (~1,400 m above sea level). In this altitudinal belt dripwaters were found to be undersaturated to slightly supersaturated with respect to calcite. It can be presumed therefore, that, in the Alpine realm, the deciduous forest upper limit can mark the usual upper boundary for active calcite precipitation. For speleothems that are found in caves above this altitude, the environmental setting at the time of speleothem formation must have been different with respect to the present. This is expected in Alpine regions that experienced several glacial-interglacial fluctuations.

Another point that must be taken into consideration, especially for the older speleothems, is that some parts of the Alpine chain, such as, for example, Altopiani Ampezzani in the Dolomites, have experienced rapid uplift of more than 1000 meters over the last 2 million years (Frisia *et al.* 1994).

Taking into account the Quaternary evolution of the area outlined above, we suggest that the opening of the system was caused by undersaturated waters that, percolating along the intercrystalline porosity, introduced ^{230}Th into the speleothems. Previous studies (Borsato 1995; Frisia 1996; Frisia *et al.* 2000) have shown that subsamples yielding (^{230}Th/^{234}U) between 1.4 and 3.4 are typically associated with zones of speleothems that either show erosion/dissolution features such as dissolutional pits or are marked by distinct microfabrics (e.g., reorganization of small individuals into larger domains; replacement of acicular crystals by patches of equant calcite spar), or both.

Molecules of organic acids, which are the most likely vehicles transporting Th in adsorbed state, are relatively large (ca. 0.5 to 10 nm for fulvic and humic acids; Buffle & Van Leeuven, 1992). Inorganic particles coated with organic compound might have even greater sizes (0.1 to 10 μm). It might be speculated that fine intercrystalline porosity of speleothems might act similarly to a filter, retarding or even immobilizing such molecules and thus introducing into the sample allogenic ^{230}Th, "unsupported" by sample's ^{238}U.

3.6. U-Th age distribution in samples from north-eastern Italy

The specimens with (^{230}Th/^{232}Th) > 20 were studied petrographically in order to look for the evidence of the opening of the system. All samples were found to consist of macrocrystalline calcite or unweathered, microcrystalline, laminated calcite (Borsato 1995; Frisia *et al.* 2000). No traces of dissolution or recrystallisation were detected. Therefore, these samples can be tentatively considered closed-system ones. From the age distribution of these 18 samples (plus 10 samples with ^{230}Th/^{232}Th activity ratio between 10 and 20) it is possible to determine that, over the last 300 ka, speleothem deposition took place during five time intervals: 0 to 10 ka, 40 to 63 ka, 88 to 100 ka, 140 to 170 ka, and 190 to 250 ka (Fig. 8). The first three periods and the last

one correlate well with positive shifts of the insolation curve (Berger & Loutre 1991) and the orbitally tuned marine oxygen isotope record (Martinson *et al.* 1987), i.e. with warmer interglacial stages.

On the contrary, the period from 140 to 170 ka is inconsistent with both the oxygen isotope record and other European growth frequencies curves (Henning *et al.* 1983; Gordon *et al.* 1989; Baker *et al.* 1993; Hercmann 2000). In fact, all records indicate an important speleothem growth phase during isotopic stage 5e, the Eemian, the dating of which is from 110.8 to 129.8 ka in marine cores (respectively event 5.4 and 6.0 in Martinson *et al.* 1987), and from 110 to 127 ka in the continental pollen record (Guiot *et al.* 1989). In our studied speleothems, the Eemian is not recorded, but three samples document a growth phase from 138 to 175 ka (1σ error), which falls within the cold isotope stage 6. These data seem to corroborate recent works (cfr. Spötl *et al.* 2002) that showed that in the Eastern Alps the start of speleothem growth after isotope stage 6 is older that predicted from ice cores data i.e. at about 135 ka.

An alternative explanation is that speleothems that yielded U-Th ages of 140 to 155 ka underwent a minor "opening" that shifted back the calculated U-Th ages by several thousand years. The latter hypothesis is difficult to prove, since neither petrographic not U-series isotope evidence provides unequivocal support to it. Yet, the amounts of ^{230}Th that need to be added to the dated specimens in order to shift ages by 20-40 ka are so tiny that the chances to detect this addition in isotopic data are slim.

4. CONCLUSION: IMPLICATIONS OF OPEN-SYSTEM BEHAVIOR FOR DATING

During the last half million years, speleothems in alpine caves were subjected to dramatic environmental changes related to glacial activity and uplifting. Many caves located near the valley bottoms have experienced invasion of turbulent meltwaters. Caves located at higher elevations as a result of uplifting by several hundred meters were moved into the different vegetation belts, which caused undersaturation of the seepage waters. It appears probable that some speleothem samples from our collection that are older than 80 ka were affected by undersaturated water flows and, consequently, experienced diagenetic modifications and geochemical opening of the U-Th system which renders the U-Th system inapplicable for dating purposes.

The detailed Quaternary geology studies of the surrounding area and thorough petrographic analyses of each speleothem sample must accompany the U-series isotope analyses in order to alert researchers regarding the possibility of the open-system behaviour of some samples. Yet, even those studies may not necessarily detect small-scale perturbations, when the affected sample remains within the calculated U-series decay field.

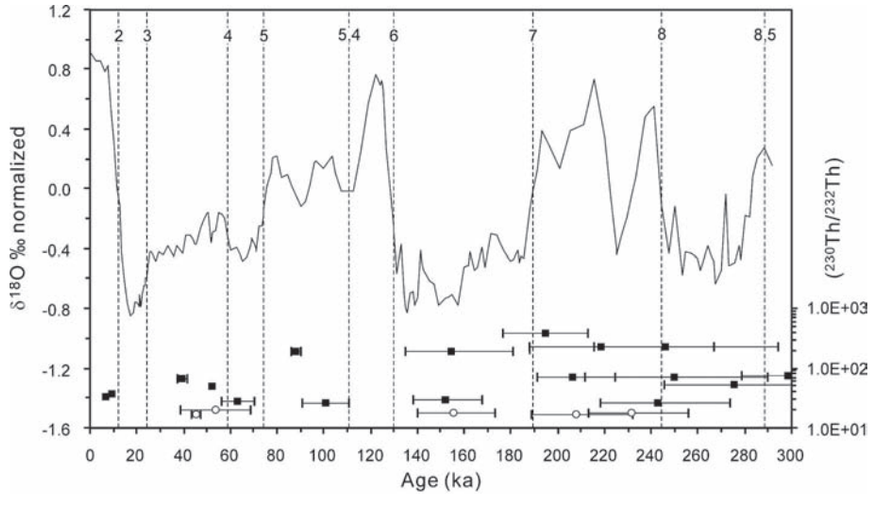

Fig. 8 - Comparison between calculated "closed" system speleothem ages (solid squares = samples with (^{230}Th/^{232}Th) >20; open circles = samples with (^{230}Th/^{232}Th) 10 to 20) and the orbitally tuned oxygen isotope record (Martinson *et al.* 1987). Numbered vertical dashed lines identify the oxygen isotope stages. The Eemian interglacial is comprised between line 5.4 and 6 (cfr. Martinson *et al.* 1987 and Guiot *et al.* 1989). Samples error bars = 1 σ.

Fig. 8 - Confronto tra le età calcolate da speleotemi di sistema "chiuso" (quadrati pieni = campioni con (^{230}Th/^{232}Th) >20; cerchi vuoti = campioni con (^{230}Th/^{232}Th) tra 10 e 20) e il record marino del δ^{18}O (Martinson et al. *1987). Le linee verticali tratteggiate identificano gli stadi isotopici. L'interglaciale Eemiano è compreso tra gli stadi 5.4 e 6 (cfr. Martinson et al. 1987 e Guiot* et al. *1989). Le barre di errore sono di 1 sigma.*

ACKNOWLEDGEMENTS

This work was supported by the Italian National Research Council CNR - Centro di Geodinamica Alpina e Quaternaria, and by the AQUAPAST project funded by the Autonomous Province of Trento. Y. Dublyansky benefited from the NEXTEC project funded by the Autonomous Province of Trento. We would like to thank Silvia Frisia, Rainer Grün, Christopher Hawkesworth, and Joyce Lundberg for critical revision of the earlier version of the manuscript.

REFERENCES

Baker A., Smart P.L. & Ford D.C., 1993 - Northwest European paleoclimate as indicated by growth frequency variations of secondary calcite deposits. *Palaeogeography, Palaeoclimatology, Palaeoecology*, 100: 291-301.

Baker A., Smart P.L. & Edwards R.L., 1995 - Paleoclimate implications of mass spectrometric dating of a British flowstone. *Geology*, 23 (4): 309-312.

Berger A. & Loutre, M.F., 1991- Insolation values for the last 10 million years. *Quaternary Science Reviews*, 10: 294-317.

Bini A. & Uggeri A., 1992 - Sedimentation en melieu periglaciaire: l'example de la Grotte Shangai (M. Campo dei Fiori, Varese, Lombardie, Italie). *Actes des Journées Pierre Chevalier*, Grenoble 1991: 118-137.

Bini A., Uggeri A. & Quinif Y., 1997 - Datazioni U/Th effettuate in Grotte delle Alpi (1986-1997): Considerazioni sull'evoluzione del carsismo e del paleoclima. *Geologia Insubrica*, 2: 31-58.

Borsato A., 1995 - *Ambiente di precipitazione e analisi microstratigrafiche di speleotemi in grotte delle Dolomiti di Brenta e Valsugana (Trento): interpretazioni genetiche e implicazioni paleoclimatiche*. Unpublished Ph.D. Thesis, University of Milano: 175 pp.

Bourdon B., Henderson G.M., Lundstrom C.C. & Turner S.P., 2003 - Introduction to U-series Geochemistry. In: Bourdon B., Henderson G.M., Lundstrom C.C. & Turner S.P. (eds), Uranium-series geochemistry. *Reviews in mineralogy and geochemistry*, 52, Geochemical Society and Mineralogical Society of America: 1-21.

Buffle J. & Van Leeuven H.P., 1992 - *Environmental particles*. Lewis Publishers, London.

Cantillana R., Quinif Y. & Maire R., 1986 - Uranium - Thorium dating of stalagmites applied to study the Quaternary of the Pyrénées (France): the example of the "Gouffre de la Pierre – Saint-Martin". *Chemical Geology*, 57: 137-144.

Cherdyntsev V.V., 1971 - Uranium 234. *Israel Programme for Scientific Translations*. Editore, Jerusalem.

Dorale J.A., González L.A., Reagan M.K., Pickett D.A., Murrell M.T. & Baker R.G., 1992 - A high-resolution record of Holocene climate change in speleothem calcite from Cold Water Cave, northeast Iowa. *Science*, 258: 1626-1630.

Fleischer R.L., 1980 - Isotopic disequilibrium of uranium: alpha-recoil damage and preferential solution effects. *Science*, 201: 979-981.

Fleisher R.L. & Raabe O.G., 1975 - Recoiling alpha-emitting nuclei. Mechanisms for uranium-series disequilibrium. *Geochim. Cosmocim. Acta*, 42: 973-978.

Ford D.C. & Williams P.W., 1989 - *Karst geomorphology and hydrology*. Unwin Hyman, London: 601 pp.

Frisia S., 1996 - Petrographic evidences of diagenesis in speleothems: some examples. *Speleochronos*, 7: 21-30.

Frisia S., Bini A. & Quinif Y., 1994 - Morphologic, crystallographic and isotopic study of an ancient flowstone (Grotta di Cunturines, Dolomites) - Implications for paleoenvironmental reconstructions. *Speleochronos*, 5: 3-18.

Frisia S., Borsato A., Fairchild I.J. & McDermott F., 2000 - Calcite fabrics, growth mechanisms, and environments of formation in speleothems from the Italian Alps and southwestern Ireland. *Journal of Sedimentary Research*, 70 (5): 1183-1196.

Frisia S., Borsato A., Fairchild I.J & Selmo E.M., 2002 - Aragonite to calcite transformation in speleothems (Grotte de Clamouse, France): environment, fabrics and carbonate geochemistry. *Journal of Sedimentary Research*, 72 (5): 687-699.

Gascoyne M., 1992 - Paleoclimate determination from cave calcite deposits. *Quaternary Science Reviews*, 11: 609-632.

Gascoyne M., Ford D.C. & Schwarcz H.P., 1978 - Uranium series dating and stable isotope studies of speleothems. Part 1: Theory and techinques. *Trans. Brit. Cave Res. Assoc*., 5: 91-112.

Gordon D., Smart P.L., Ford D.C., Andrews J.N., Atkinson T.C., Rowe P.J. & Cristopher N.J., 1989 - Dating of Late Pleistocene interglacial and interstadial periods in the United Kingdom from speleothem growth frequency. *Quaternary Research*, 31: 14-26.

Guiot J., Pons A., Beaulieu J.L. & Reille M., 1989 - A 140000 year continental climate reconstruction from two European pollen records. *Nature*, 338: 309-313.

Harmon R.S., Thompson P., Scwarcz H.P. & Ford D.C., 1975 - Uranium-series dating of speleothems. *Bullettin of the National Speleological Society*, 37: 21-33.

Henning G.J., Grun R. & Brunnacher K., 1983 - Speleothems, travertines and paleoclimates. *Quaternary Research*, 29: 1-29.

Hercmann H., 2000 - Reconstruction of paleoclimatic changes in Central Europe between 10 and 200 ka BP, base on analysis of growth frequencies of speleothems. *Studia Quat.*, 17: 35-70.

Hill C.A. & Forti P., 1997 - *Cave Minerals of the World.* Natl. Speleol. Soc. Inc. Huntsville, Alabama: 464 pp.

Ivanovich M. & Alexander J., 1987 - Application of uranium-series disequilibrium to studies of groundwater mixing in the Harwell region, UK. *Chem. Geol*., 66: 279-291.

Kersting A.B., Efurd D.W., Finnegan D.L., Rokop D.J., Smith D.K. & Thompson J.L., 1999 - Migration of plutonium in ground water at the Nevada Test Site. *Nature*, 397: 56-59.

Langmuir D. & Herman J.S., 1980 - The mobility of thorium in natural waters at low temperatures. *Geochim. Cosmocim. Acta*, 44: 547-569.

Lauritzen S.E., Ford D.C. & Schwarcz H.P., 1986 - Humic substances in speleothem matrix – Paleoclimatic significance. In: *9th Int. Congr. Speleol. Barcelona*, 2: 77-79.

Maire R., 1990 - La haute montaigne calcaire. *Karstologia, Memoires*, 3.

Martinson D.G., Pisias N.G., Hays J.D., Imbrie J., Moore T.C. & Shackleton N.J., 1987 - Age dating and the orbital theory of the Ice age: developement of a high-resolution zero to 300,000-year chronostratigraphy. *Quaternary Research*, 27: 1-29.

McDermott F., Frisia S., Yiming H., Longinelli A., Spiro B., Heaton T.H.E., Hawkesworth C.J., Borsato A., Keppens E., Fairchild I.J., van der Borg K., Verheyden S. & Selmo E., 1999 - Holocene climate variability in Europe: evidence from $\delta^{18}O$, textural and extension-rate variations in three speleothems. *Quaternary Science Reviews*, 18: 1021-1038.

Osmond J.K. & Cowart J.B., 1982 - Ground water. In: Ivanovich M. & Harmon R.S. (eds), *Uranium series disequilibrium. Applications to environmental problems*. 1° ed., Clarendon Press, Oxford: 259-289.

Railsback B.L., Dabous A.A., Osmond J.K. & Fleisher C.J., 2002 - Petrographic and geochemical screening of speleothems for U-series dating: An example from recrystallized speleothems from Wadi Sannur Cavern, Egypt. *Journal of Cave and Karst Studies*, 64 (2): 108-116.

Ramseyer K., Miano T.M., D'Orazio V., Wildberger A., Wagner T. & Geister J., 1997 -Nature and prigin of organic matter in carbonates from speleothems, marine cements and coral skeletons. *Org. Geochem*., 26 (5/6): 361-378.

Reeder R.J., Nugent M., Tait D., Morris D.E, Heald S.M., Beck K.M., Hess W.P. & Lanzirotti A., 2001 - Coprecipitation of Uranium (VI) with Calcite: XAFS, micro-XAS, and luminescence characterization. *Geochim. Cosmocim. Acta*, 65 (20): 3491-3503.

Richards D.A. & Dorale J.A., 2003 - Uranium-series chronology and environmental applications of speleothems. In: Bourdon B., Henderson G.M., Lundstrom C.C. & Turner S.P. (eds), Uranium-series geochemistry. *Reviews in mineralogy & Geochemistry*, 52: 407-460.

Sauro U. & Meneghel M. (eds), 1995 - *Altopiani Ampezzani: geologia, geomorfologia, speleologia*. La Grafica Editrice, Padova: 156 pp.

Shopov Y.Y., Ford D.C. & Schwarcz H.P., 1994 - Luminescent microbanding in speleothems: High-resolution chronology and paleoclimate. *Geology*, 22: 407-410.

Spötl C., Mangini A., Frank N., Eichstädter R. & Burns S.J., 2002 - Start of the last interglacial period at 135 ka: Evidence from a high Alpine speleothem. *Geology*, 30 (9): 815-818.

Uggeri A., 1992 - *Analisi geologico ambientale di un massiccio carbonatico prealpino (M. Campo dei Fiori, Varese): geologia, geologia del Quaternario, Idrogeologia.* Unpublished Ph.D. Thesis, University of Milano.

Uggeri A., Bini A. & Quinif Y., 1991 - Datation des sédiments de la Grotte Marelli. *Speleochronos*, 2: 21-28.

Uggeri A., Bini A. & Quinif Y., 1992 - Contribution of isotope geochemistry to the study of climatic and environmental evolution of Monte Campo dei Fiori (Lombardy, Italy). *Speleochronos*, 3: 17-28.

White B.W. & Brennan E.S., 1989 - Luminescence of speleothems due to fulvic acid and other activators. In: 10th Int. Congr. Speleol., Budapest, 1: 212-214.

Whitehead N.E., Ditchburn R.G., Williams P.W. & McCabe W.J., 1999 - 231 Pa and ^{230}Th contamination at zero age: a possible limitation on U/Th series dating of speleothem material. *Chemical Geology*, 156: 359-366.